Ecosystems (2023) 26: 826–842
https://doi.org/10.1007/s10021-022-00801-5
© 2022 The Author(s), under exclusive licence to Springer Science+Business Media, LLC, part of Springer Nature
ECOSYSTEMS

Sedimentary Organic Carbon and Nitrogen Sequestration Across a Vertical Gradient on a Temperate Wetland Seascape Including Salt Marshes, Seagrass Meadows and Rhizophytic Macroalgae Beds

Carmen B. de los Santos,[1]* Luis G. Egea,[2] Márcio Martins,[1] Rui Santos,[1] Pere Masqué,[3,4] Gloria Peralta,[2] Fernando G. Brun,[2] and Rocío Jiménez-Ramos[2]

[1]*Centre of Marine Sciences of Algarve, Faro, Portugal;* [2]*Department of Biology, University of Cádiz, Puerto Real, Cádiz, Spain;* [3]*International Atomic Energy Agency, Principality of Monaco, Monaco;* [4]*School of Science and Centre for Marine Ecosystems Research, Edith Cowan University, Joondalup, Australia*

Abstract

Coastal wetlands are key in regulating coastal carbon and nitrogen dynamics and contribute significantly to climate change mitigation and anthropogenic nutrient reduction. We investigated organic carbon (OC) and total nitrogen (TN) stocks and burial rates at four adjacent vegetated coastal habitats across the seascape elevation gradient of Cádiz Bay (South Spain), including one species of salt marsh, two of seagrasses, and a macroalgae. OC and TN stocks in the upper 1 m sediment layer were higher at the subtidal seagrass *Cymodocea nodosa* (72.3 Mg OC ha^{-1}, 8.6 Mg TN ha^{-1}) followed by the upper intertidal salt marsh *Sporobolus maritimus* (66.5 Mg OC ha^{-1}, 5.9 Mg TN ha^{-1}), the subtidal rhizophytic macroalgae *Caulerpa prolifera* (62.2 Mg OC ha^{-1}, 7.2 Mg TN ha^{-1}), and the lower intertidal seagrass *Zostera noltei* (52.8 Mg OC ha^{-1}, 5.2 Mg TN ha^{-1}). The sedimentation rates increased from lower to higher elevation, from the intertidal salt marsh (0.24 g cm^{-2} y^{-1}) to the subtidal macroalgae (0.12 g cm^{-2} y^{-1}). The organic carbon burial rate was highest at the intertidal salt marsh (91 ± 31 g OC m^{-2} y^{-1}), followed by the intertidal seagrass, (44 ± 15 g OC m^{-2} y^{-1}), the subtidal seagrass (39 ± 6 g OC m^{-2} y^{-1}), and the subtidal macroalgae (28 ± 4 g OC m^{-2} y^{-1}). Total nitrogen burial rates were similar among the three lower vegetation types, ranging from 5 ± 2 to 3 ± 1 g TN m^{-2} y^{-1}, and peaked at *S. maritimus* salt marsh with 7 ± 1 g TN m^{-2} y^{-1}. The contribution

Received 17 June 2022; accepted 8 October 2022;
published online 28 October 2022

Supplementary Information: The online version contains supplementary material available at https://doi.org/10.1007/s10021-022-00801-5.

Author contribution: CBdlS: Conceptualization, Methodology, Formal analysis, Investigation, Data curation, Visualization, Writing—original draft, Funding acquisition, Resources. LGE: Conceptualization, Investigation, Writing – review and edit, Funding acquisition, Resources. MM: Methodology, Investigation, Visualization, Writing – review and edit. PM: Methodology, Formal analysis, Resources, Writing – review and editing. FGB: Resources, Writing – review and edit. GP: Resources, Visualization, Writing – review and edit. RS: Investigation, Resources, Writing – review and edit. RJ-R: Conceptualization, Methodology, Investigation, Writing – review and edit, Funding acquisition, Resources.

**Corresponding author; e-mail:* cbsantos@ualg.pt

of allochthonous sources to the sedimentary organic matter decreased with elevation, from 72% in *C. prolifera* to 33% at *S. maritimus*. Our results highlight the need of using habitat-specific OC and TN stocks and burial rates to improve our ability to predict OC and TN sequestration capacity of vegetated coastal habitats at the seascape level. We also demonstrated that the stocks and burial rates in *C. prolifera* habitats were within the range of well-accepted blue carbon ecosystems such as seagrass meadows and salt marshes.

Key words: seascape; blue carbon; seagrass; salt marsh; Cádiz bay; caulerpa.

Highlights

- Vegetated habitats along the seascape differed in C and N burial and storage capacity
- Tidal position plausibly explains the source of allochthonous organic matter
- *Caulerpa prolifera* presented stock and burial rates similar to well-accepted blue carbon habitats

Introduction

Vegetated coastal habitats including salt marshes, mangrove forests, and seagrass meadows, are globally important carbon sinks, referred to as blue carbon ecosystems (Nellemann and others 2009). The rates of carbon sequestration in these ecosystems are exceptionally high in comparison to terrestrial ecosystems due to high rates of organic matter input, including both autochthonous primary production (Duarte and others 2010; Mcleod and others 2011) and allochthonous organic matter trapped by their canopy (Kennedy and others 2010; Mueller and others 2019), which co-occur with slow rates of organic matter decomposition (Mateo and others 1997; Duarte and others 2005; Bridgham and others 2006). This yields substantial carbon accumulation rates of, on average, 24 g C m^{-2} y^{-1} for seagrasses (95% confidence interval of 20–30 g C m^{-2} y^{-1}; Arias-Ortiz 2019) and 218 ± 24 g C m^{-2} y^{-1} for salt marshes (range of 18–1713 g C m^{-2} y^{-1}; Mcleod and others 2011), evidencing that, per unit area, these ecosystems are effective carbon sinks.

Like salt marshes and seagrasses, benthic macroalgal kelp forests are also important primary producers in the oceans (Watanabe and others 2020) that have been recently recognised as important carbon sinks as well, through the export and burial of their biomass in deep sea sediments (Krause-Jensen and Duarte 2016; Krause-Jensen and others 2018; Smale and others 2018). On the other hand, macroalgae beds that develop in soft sediments, such as several species of *Gracilaria* and *Caulerpa* genera, have been widely ignored as blue carbon ecosystems, even though they occupy extensive shallow sheltered coastal areas. In particular, the genus *Caulerpa* is widely distributed from the circum-tropical to the warm temperate bioregions (Zubia and others 2020). Species of this genus are rhizophyte algae, presenting a prostate axis or stolon with rhizoids that anchor in unconsolidated or hard substrates, and from which arise photosynthetic fronds in a diverse array of morphologies (Zubia and others 2020). *Caulerpa* beds may occur from intertidal to deep subtidal areas and, in many cases, such as for *C. prolifera* or *C. taxifolia*, the beds cover large areas over the whole year, exhibiting seasonal biomass patterns in warm temperate locations (Vergara and others 2012).

The Paris Agreement includes carbon sequestration in the strategies to attain a 50% reduction of CO_2 emissions by 2030, to keep the global mean temperature below 1.5 °C increase. These strategies include the preservation and restoration of ecosystems that act as natural carbon sinks. However, the accounting of carbon sequestration by natural coastal and marine macrophyte habitats remains a challenge, mainly due to the high spatial variability in carbon stocks and burial rates that can even be observed in a single system (for example, Martins and others 2021; Ricart and others 2020). Therefore, a substantial increase in the available data of organic carbon stocks and sequestration rates of these important ecosystems is still needed (Macreadie and others 2019).

The sequestration rate and long-term storage of nutrients by vegetated coastal ecosystems is equally important as nutrient pollution and eutrophication are major environmental threats to coastal ecosystems (Rabalais and others 2009). Both seagrasses and salt marshes are efficient at removing nutrients from the water column and burying them in the sediment in the form of organic matter, similarly as explained for the organic carbon (for example, Romero and others 1999; Sousa and others 2017; Santos and others 2019; Martins and others 2021). The role of vegetated coastal ecosystems in nitrogen sequestration is another highly valuable ecosystem service, particularly because the market price for

nitrogen removal is much higher than that for carbon (for example, Cole and Moksnes 2016).

Studies on carbon and nitrogen stocks in temperate coastal areas commonly focus on single habitats such as seagrasses or salt marshes (for example, Sousa and others 2017, 2019), whereas the seascape vertical variation, including the subtidal macroalgae beds, common in many systems, is largely overlooked. Habitat diversity and interconnectivity are important factors in blue carbon sequestration (Huxham and others 2018; Bulmer and others 2020) and so must be for nitrogen sequestration. Part of the carbon and nitrogen exported by the seascape habitats fuels community metabolism in neighbouring habitats, while another part is stored as allochthonous organic matter in their sediments, accounting for as much as the 50% of the sediment carbon (Kennedy and others 2010). Understanding differences in carbon and nitrogen stocks and sequestration rates across habitats along the seascape is important for global accounting and for estimating the effects of habitat changes (for example, due to sea level rise or restoration efforts) in the provision of coastal ecosystem services. The distribution of vegetated habitats across the vertical gradient in the seascape is mostly driven by the bed elevation, since the occurring of plant communities depends on the tidal flooding regime through their limits in inundation and salinity tolerance (for example, Pennings and Callaway 1992).

Here we investigated the carbon and nitrogen stocks and sequestration rates, and the organic matter sources at four adjacent vegetated coastal habitats occurring in the vertical gradient of a temperate seascape in Cádiz Bay (southern Spain), from the upper intertidal to shallow subtidal: the halophyte *Sporobolus maritimus*, the seagrasses *Zostera noltei* and *Cymodocea nodosa*, and the green rhizophytic macroalga *Caulerpa prolifera*. The specific research questions were: (1) how do carbon and nitrogen stocks and sequestration rates vary among the vegetated habitats in the same seascape? and (2) how do the autochthonous and allochthonous contributions of organic matter to the sediments vary among habitats? We hypothesised that the higher immersion time of subtidal habitats results in a higher trapping of allochthonous particulate matter to the sediment organic matter pool, and to a lower exposure to air-exposed remineralization conditions, resulting in higher sedimentary carbon and nitrogen stocks and burial rates than in intertidal habitats.

Materials and Methods

Study Area and Sampling

The study was conducted in Cádiz Bay, southern Spain (36.47° N, 6.25° W; Figure 1A). Cádiz Bay is divided in two water bodies (inner and outer bays) subject to a mesotidal semi-diurnal regime, with a maximum tidal range of 3.5 m (Álvarez and others 1999). The inner bay is a shallow environment with a mean 2 m LAT depth (relative to the Lowest Astronomical Tide), sheltered from the action of oceanic waves and with dominant sediment composition of silt and clay (Carrasco and others 2003). Water exchange mainly occurs through a narrow strait that connects the inner and the outer basins and an extensive system of creeks and channels connecting the bay to the surrounding salt marshes. Tidal water exchange is high, with up to 75% of water column renovation during the tidal cycle (Álvarez and others 1999).

Plant zonation in the inner bay, frow lowest to highest elevation, includes extensive beds of the rooting macroalgae *Caulerpa prolifera* (Forsskål) J. V. Lamouroux (Morris and others 2009) at subtidal elevations; a fringe of *Cymodocea nodosa* Ucria (Ascherson) meadows (Peralta and others 2021), with few discrete patches of *Zostera marina* Linnaeus (Brun and others 2015), from subtidal to low intertidal elevations; meadows of seagrass *Z. noltei* Hornem. in the lower intertidal area; and patches of the saltmarsh plant *Sporobolus maritimus* (Curtis) P.M. Peterson and Saarela in the upper intertidal (Figure 1).

Surrounded by 5 cities, Cádiz Bay is highly urbanised and affected by anthropogenic impacts (de Andrés and others 2018), such as high nutrient inputs from aquaculture and, in the past, urban discharges (Morris and others 2009). Despite these anthropogenic pressures, the quality of the system is still high and most intertidal areas of the natural area of Cádiz Bay are protected as a Natural Park (Law 2/1989/CA), a RAMSAR site (1265, 24/10/02), a SCI and SPA sites (Birds Directive 79/409/CEE, ES0000140 2006/613/CE); and the subtidal areas as SCIs integrated into the Nature 2000 Network (ES6120009, EU Habitats Directive 92/43/CEE, 2006/613/CE).

The inner bay habitats of the intertidal saltmarsh plant *Sporobolus maritimus*, the intertidal seagrass *Zostera noltei*, the subtidal seagrass *Cymodocea nodosa*, and the subtidal macroalgae *Caulerpa prolifera* were sampled with sediment cores along the elevation gradient, at the area known as Santibañez on 22

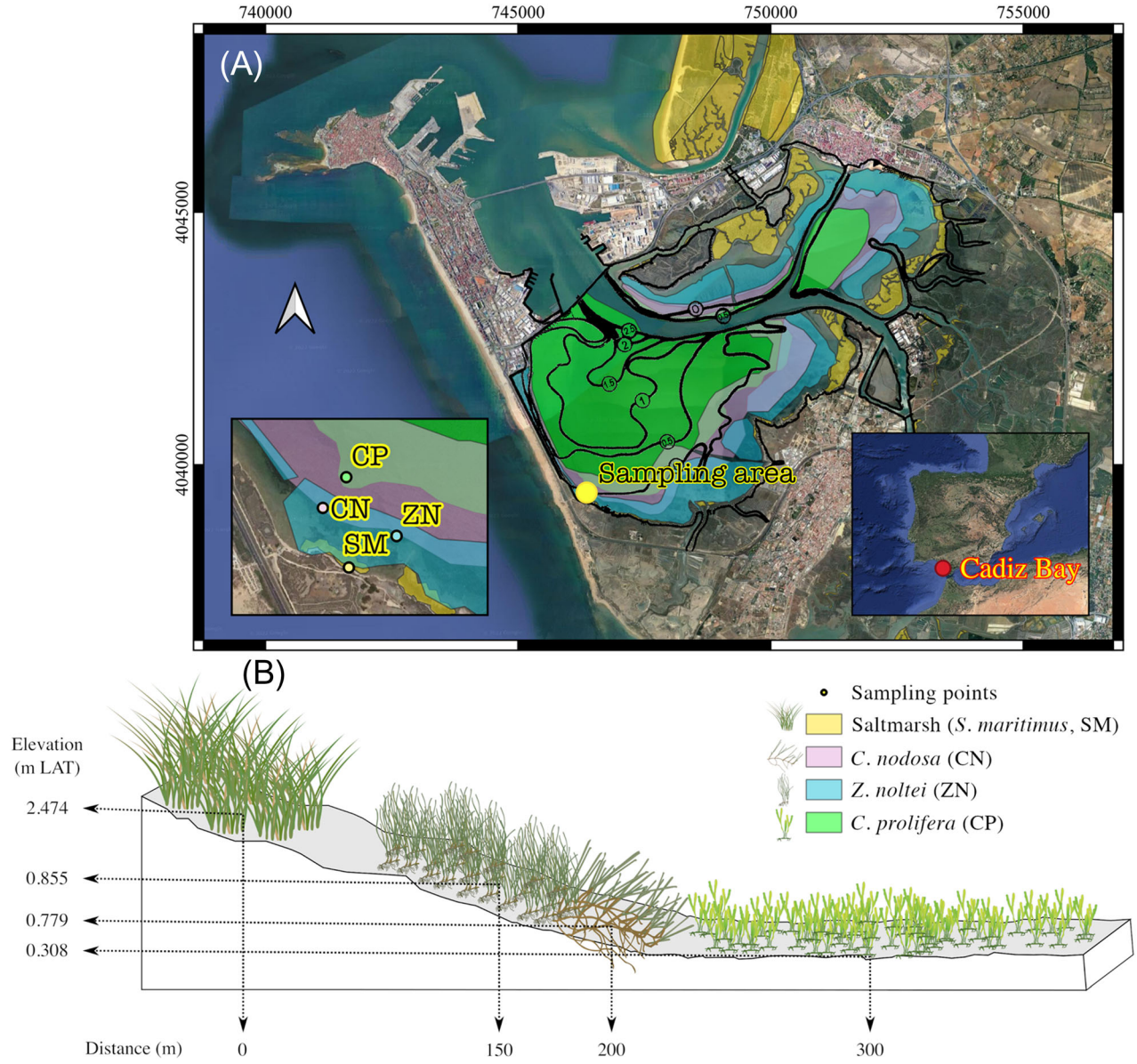

Figure 1. **A** Overview of the inner waterbody of Cádiz Bay with distribution of dominant vegetation, depth isolines (m), and location of the sampling points. **B** Detailed distribution of the sampling points along the elevation gradient at the seascape level. Elevation is expressed with respect to the Lowest Astronomical Tide (LAT). The map projected in EPSG:25829 using the easting/northing terminology, with scale frame representing 5-km units. Source of satellite image: Google Satellite. Source of macrophyte distribution maps: modified from Muñoz-Pérez and Sánchez de Lamadrid (1994). Icons: IAN symbols.

February 2018 (Figure 1B, Table 1). The cores, one per habitat, were collected using manual percussion and rotation (PVC pipe, 170 cm length, 48 mm internal diameter), with a penetration depth ranging from 79 to 122 cm (Table 1). We assumed that the sampled sediment core throughout the depth profile corresponds to the present habitat; however, we do not have historical data to be sure that this is the case. Sediment compaction during coring was considered linear and was measured based on the total length of the corer, the empty space inside the corer with the sediment sample in before retrieval, and the length of sediment retrieved, and it ranged from 31 to 44% (Table 1). All results presented hereafter refer to equivalent decompressed depths. After extraction, the corers were sealed at both ends to avoid sediment loss and air exposure, transported to the laboratory in vertical position, and immediately cut longitudinally into two halves for sub-sampling.

Table 1. Information on the Sampling Sites and Sediment Cores Collected in the Four Vegetated Habitats at the Seascape: *Sporobolus maritimus*, *Zostera noltei*, *Cymodocea nodosa*, and *Caulerpa prolifera*

Variable	Salt marsh *Sporobolus maritimus*	Seagrass *Zostera noltei*	Seagrass *Cymodocea nodosa*	Macroalgae *Caulerpa prolifera*
Latitude (EPSG:4326, °)	36.467	36.468	36.469	36.470
Longitude (EPSG:4326, °)	− 6.251	− 6.249	− 6.252	− 6.251
Easting (EPSG:25829, m)	746,319	746,495	746,223	746,310
Northing (EPSG:25829, m)	4,039,261	4,039,377	4,039,480	4,039,594
Elevation (m LAT)	2.474	0.855	0.779	0.308
Horizontal distance (m)	0	150	200	300
Penetration depth (cm)	79	122	116	122
Compaction (%)	31	33	33	44
Depth of distinct deposit (cm)	47–70	55–80	65–116	93–122

LAT Lowest Astronomical Tide. Horizontal distance refers to the distance from the sampling point at the Sporobolus maritimus *salt marsh (the highest elevation) to the other sampling points. The distinct deposit was a layer found in the four habitats characterised by the presence of pebbles, shells and/or coral fragments (see text for details).*

Above-ground biomass of *S. maritimus*, *Z. noltei*, *C nodosa*, and *C. prolifera* (fronds) were sampled (n = 3) at each sampling point for isotopic characterization, including old tissues. Water samples were also collected nearby the subtidal sampling points and filtered with a syringe (GF/F 47-mm) to obtain suspended particulate organic matter (POM) samples (n = 3). Samples were transported to the laboratory in cool, dark conditions, and macrophytes were gently cleaned with distilled water, dried (60 °C), and homogenized in a ball grinder for further analysis.

Geochemical Analysis and Quantification of Organic Carbon and Total Nitrogen Stocks and Sequestration Rates

The sediment cores were opened lengthwise with an angle grinder and the sediment profile was visually inspected to define the main layers according to colour and grain size. From one half core sediment samples were extracted with a plastic syringe at 2-cm thick intervals, frozen at -20 °C, lyophilized (24 h), and weighted (dry weight, dw, ± 0.0001 g) to determine the dry bulk density (DBD, g dw cm^{-3}) (sample size: n = 39 for *C. nodosa*, n = 34 for *C. prolifera*, n = 27 for *S. maritimus*, n = 40 for *Z. noltei*; total n = 140). Samples were then ground to fine powder (Fritsch planetary ball mill, using agate material) and subdivided into two subsamples for loss-on-ignition (LOI) (A subsample) and elemental and isotopic analyses (B subsample). LOI analysis (450 °C, 4 h) was conducted on all A subsamples to obtain the content of organic matter (OM, % dw). Subsequently, a selection of subsamples A (all samples from the top 15 cm and at the beginning and end of each visually identified layer, n = 80) were subjected to LOI at 950 °C (2 h) to obtain the $CaCO_3$ content (% dw). Following the same selection as for $CaCO_3$ analysis, B subsamples (*ca.* 10 mg dw) were used for elemental and isotopic determination using a ratio mass spectrometry-elemental analyser at the UH Hilo Analytical Laboratory, USA. Organic carbon content (OC, % dw) and $\delta^{13}C$ (‰ vs. Vienna Pee Dee Belemnite, VPDB) were determined after removal of inorganic carbon by addition of 1 M HCl (Kennedy and others 2005). Bulk OC content (pre-acidification) was calculated after applying a correction factor for the mass lost during acidification. Total nitrogen content (TN, % dw) and $\delta^{15}N$ (‰ vs. air) were determined on non-acidified samples due to the high carbonate contents in the samples (Peng and others 2018). Two quality control reference samples (NIST 8704, Buffalo River Sediment) were run with the sediment samples, and a two-point calibration was used to normalize the data using standards USGS40 and USGS41, yielding an accuracy of 0.2 ‰.

Linear relationships between OM and OC and between OM and TN were fitted to the data of each habitat (Figure S1, Table S1) because exploratory analysis revealed significant differences among them. When the intercept of the linear regression was not significant, it was forced to equal zero.

These equations were used to estimate the OC and TN contents in the rest of the samples (n = 60). Sediment stocks of OC and TN (g cm^{-2}) were estimated by multiplying OC or TN contents (g OC or TN g^{-1} dw) by DBD (g dw cm^{-3}), and by integrating the products over depth (0.75 and 1 m) following standards techniques (Howard and others 2014). In the *S. maritimus* core, sediment length was less than 1 m (0.79 m), and thus the OC and TN contents of the deepest available sample were assumed constant down to 1 m to obtain the 1-m stock.

The second core half was sliced and sampled at 1-cm thick regular intervals (excluding the sediments near the wall of the corer to avoid cross-contamination due to smearing) for ^{210}Pb dating analysis to estimate the sediment accumulation rates. The concentration of ^{210}Pb along the upper layers of the sediment cores were determined through the analysis of its decay product ^{210}Po, in equilibrium with ^{210}Pb, by alpha spectrometry after acid-digested in an analytical microwave in the presence of ^{209}Po as an internal tracer, following Sánchez-Cabeza and others (1998). Excess concentrations of ^{210}Pb to be used to obtain the age-depth models were calculated as the difference between total ^{210}Pb and ^{226}Ra. Supported ^{210}Pb was determined by analysis of ^{226}Ra by gamma spectrometry in selected samples of each core. The Constant Rate of Supply (CRS; Appleby and Oldfield 1978) and Constant Flux:Constant Sedimentation (CF:CS; Krishnaswamy and others 1971) models were applied, when possible, following the recommendations in Arias-Ortiz and others (2018). Sediment accumulation rate (SAR, mm y^{-1}; corrected for compression) and mass accumulation rate (MAR, g cm^{-2} y^{-1}) were estimated from the applied model in each case. Although the ^{210}Pb dating technique allowed us to determine the accumulation rates in the *Z. noltei* and *C. nodosa* cores, it could not be used to obtain and age-depth models in the *S. maritimus* and *C. prolifera* cores, due to the likeliness of sediment mixing in the upper layers. Sediment mixing is common in coastal vegetated ecosystems, which can be disturbed by natural and anthropogenic processes, resulting in sediment mixing and changes in sedimentation or erosion rates (Arias-Ortiz and others 2018). As an alternative method, the presence of a specific deposit of coarse grains, pebbles, and bioclasts (fragments of corals and mollusc shells, Figure 2) present in the four cores, allowed a historical reconstruction. This type of deposits is common in Cádiz Bay (Gutiérrez-Mas and others 2009), generally attributed to the tsunami that hit Cádiz coast in 1755 after the Lisbon earthquake. For the historical reconstruction method, the SAR was estimated by dividing the length of the sediment column above the coarse deposit by 263 years, which is the time interval between the tsunami and the core sampling. The MAR was assumed to be constant since the tsunami and was estimated by dividing the mass of the column above such deposit by the sampled area and the time interval since the tsunami. The average SAR and MAR at each habitat were calculated as the average of those obtained by both methods (*Z. noltei* and *C. nodosa*) or only by the reconstruction method (*S. maritimus* and *C. prolifera*).

OC and TN burial rates (g m^{-2} y^{-1}) were calculated as the product of the MAR (g m^{-2} y^{-1}) and the weighted average of the concentrations of OC or TN (g g^{-1} dw) along the core, using as maximum depth the one corresponding to two ages in each case: 50 and 100 years.

Determination of Organic Matter Sources in the Sediment

Stable Isotope Mixing Models were used to estimate the contributions of autochthonous (the dominant macrophyte species in each habitat) and allochthonous (particulate organic matter, POM, in the water column) sources to the sedimentary OM pool (Kennedy and others 2010). The models were initially run with 2 tracers, δ^{13}C and δ^{15}N, yet the high variability and overlapping found in the δ^{15}N signatures led us to exclude it (Figure S2). Thus, each model included 2 sources and 1 isotope (Parnell and others 2013). The isotopic signatures of the OM sources were obtained from in situ collected samples and from previously collected data at Cádiz Bay (Morris and others 2009 and authors' unpublished data) (Table 2). Only sediment samples corresponding to the last century were included in the analysis (n = 6 for *S. maritimus*, n = 7 for *Z. noltei*, n = 9 for *C. nodosa*, and n = 8 for *C. prolifera*). The δ^{13}C profiles along the sediment corresponding to the last century were generally constant in each core (yet it varied slightly in *C. nodosa*), supporting the assumption that the present vegetated habitats have not change substantially during this time frame.

The probability of relative OM contribution of each source (estimated contribution) to the corresponding sediment OM stock was evaluated with the use of Stable Isotope Mixing Models in R fed with the isotopic signatures of the sediment sam-

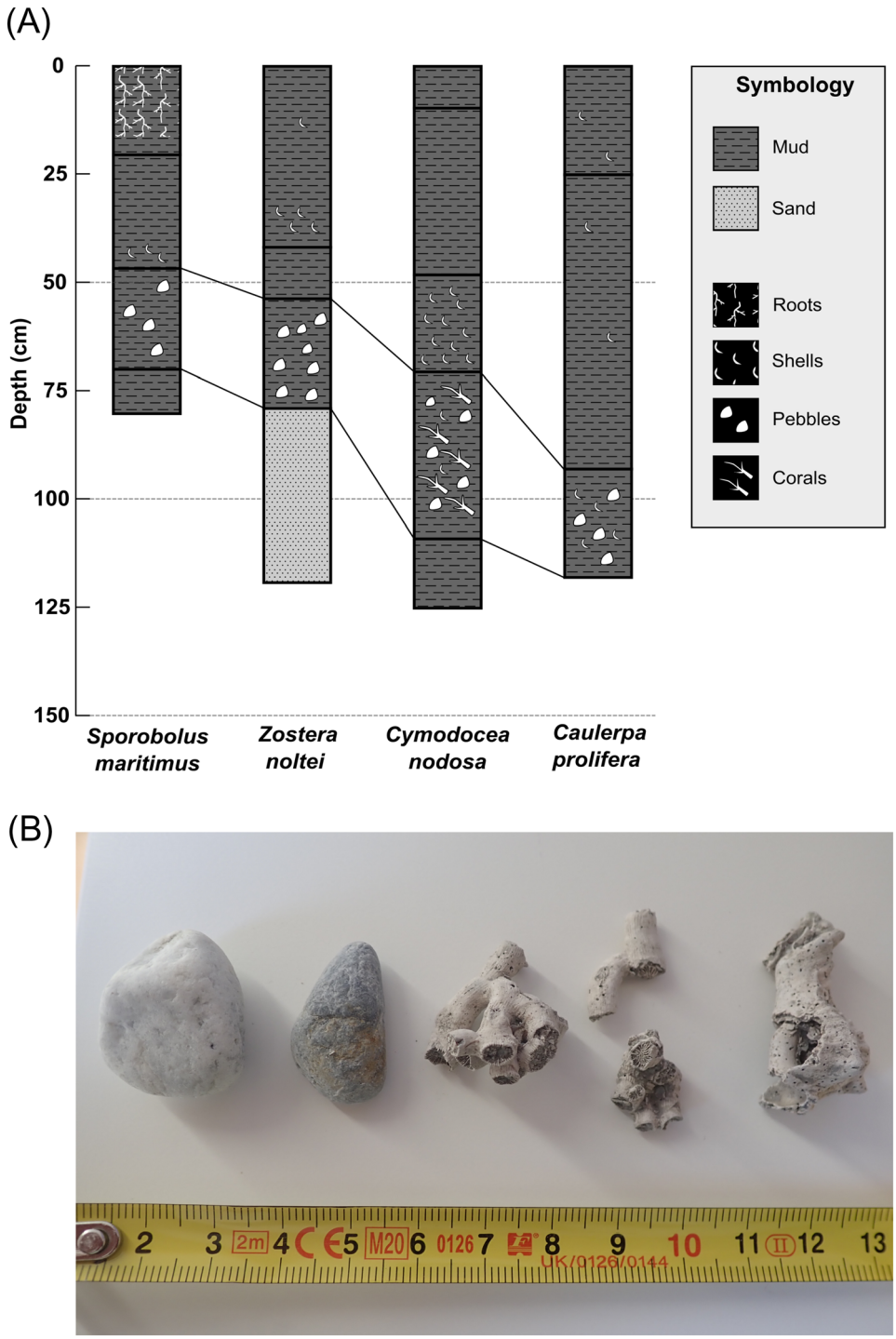

Figure 2. **A** Depth profiles of the sediment cores in the four vegetated habitats along the seascape showing the main grain-size category and presence of roots, shells, pebbles, and corals. The black lines connecting the cores highlight the distinct layer. **B** Examples of pebbles, coral fragments (*Cladocora caespitosa*), and shells found in the distinct layer of the core extracted at the *Cymodocea nodosa* habitat.

ples (''mixtures'') and of the potential sources (''simmr'' package, version 0.3; Parnell 2019). Markov Chain Monte Carlo simulations (chain length of 100,000, burn-in size of 50,000, thinning amount of 50 and 3 chains) were carried out to obtain the OM contributions. Model convergence was checked using diagnostic plots and upper confidence levels.

Table 2. Stable-isotope Signatures of the Five Sources of Organic Matter (Dominant Macrophytes and Particulate Organic Matter) Along the Landscape in the Sampling Location

Source	*n*	δ^{13}C (‰ vs. VPDB)	δ^{15}N (‰ vs. air)
Sporobolus maritimus	3	− 13.78 ± 0.33	4.51 ± 0.48
Zostera noltei	14	− 11.21 ± 1.37	8.36 ± 1.80
Cymodocea nodosa	27	− 9.27 ± 0.94	5.39 ± 2.02
Caulerpa prolifera	37	− 13.21 ± 1.43	6.50 ± 1.34
Particulate organic matter (POM)	3	− 17.72 ± 1.02	5.70 ± 0.26

Data Analysis

Data are presented as mean and standard error (or weighted mean and standard error when needed). One-way ANOVAs were used to test for differences among habitat types (fixed factor, four levels: intertidal saltmarsh *Sporobolus maritimus*, intertidal seagrass *Zostera noltei*, subtidal seagrass *Cymodocea nodosa*, and subtidal macroalgae *Caulerpa prolifera*) in sediment variables along the cores (dry bulk density, stable isotope signatures and contents of OM, $CaCO_3$, TC, OC, TN), for the upper 1-m sediment. Normality (Shapiro–Wilk test) and homoscedasticity (Fligner-Killeen test) were checked on data and variables were transformed (natural logarithm or square-root) when necessary to meet ANOVA assumptions. When differences were significant, Tukey HSD post hoc tests were carried out to assess pairwise differences between habitats. When ANOVA assumptions were not achieved even with data transformation, the comparison among habitats was performed by nonparametric Kruskal–Wallis rank sum tests, followed by Dunn's post hoc tests with Bonferroni correction, when differences among habitats were found. A significance level of 0.05 was considered for all tests. Statistical analyses were performed in the R programming language (version 4.1.2; R Core Team 2021) and RStudio software (version 2021.09.2). The dataset generated for this study is available at https://doi.org/10.5281/zenodo.7182581.

Results

According to visual inspections, the sediment was mainly composed of mud, with a deeper layer of sand in *Zostera noltei* (Figure 2A). A distinct layer with pebbles and abundant shells was observed in the four cores at 93–122 cm in *Caulerpa prolifera*, 65–116 cm in *Cymodocea nodosa*, 55–80 cm in *Z. noltei*, and 47–70 cm in *Sporobolus maritimus*. The depth of occurrence of the distinct layer decreased with increasing habitat elevation (Figure 2A). Several fossil fragments were found in the distinct layer of the *C. nodosa* core, and they were identified as *Cladocora caespitosa* (Figure 2B; J.I. Santisteban, personal communication), a common colonial scleractinian zooxanthellae coral native of the Mediterranean Sea.

The biogeochemical properties in the upper metre of sediment differed significantly among the four vegetation types, except for δ^{15}N (Table 3). DBD increased from subtidal (lighter sediment) towards the upper intertidal (heavier sediment) habitats and OM, TC, and $CaCO_3$ contents were significantly higher in the subtidal habitats (*C. prolifera* and *C. nodosa*) than in the intertidal ones (*Z. noltei* and *S. maritimus*). The seascape patterns in the contents of OC and TN were similar to those of OM, TC and $CaCO_3$, yet the contents at *C. nodosa* habitat were not significantly different from the intertidal habitats (Table 3). Sediment δ^{13}C were not significantly different among habitats except in *C. nodosa* where it was lower, while sediment δ^{15}N was similar in all the habitats. DBD generally increased along the sediment depth profile (Figure 3) in all the habitats, whereas OM, TC, OC, TN and $CaCO_3$ contents decreased, especially below the 25–50 cm sediment layer. The pattern of variation with depth was generally less pronounced in *C. prolifera* sediments, and the *S. maritimus* habitat had a relative maximum in most variables at a depth of about 15 cm (Figure 3).

The largest OC stock in the upper 1 m sediment layer was observed for the subtidal seagrass *C. nodosa*, followed by the intertidal saltmarsh plant *S. maritimus* and the subtidal rhizophytic macroalgae *C. prolifera*, with the lowest stock observed for the intertidal seagrass *Z. noltei* (Figure 4, Table 4). TN stocks followed a similar pattern and were about one order of magnitude lower than OC stocks. When calculated for the upper 0.75 m of the sediment, OC stocks were higher in the *C. nodosa* and *S. maritimus* habitats than in the *Z. noltei* and *C. prolifera* habitats, while TN stock peaked at *C. nodosa* and was similar in the other habitats (Figure 4, Table 4).

No decreasing trend of the concentrations of excess ^{210}Pb with depth could be observed in the

Table 3. Weighted Mean and Standard Error (SE) of Sediment Properties Along the Upper 1-m Sediment Layer at the Four Vegetated Habitats Along the Seascape: *Sporobolus maritimus*, *Zostera noltei*, *Cymodocea nodosa*, and *Caulerpa prolifera*

Variable	Salt marsh *Sporobolus maritimus*	Seagrass *Zostera noltei*	Seagrass *Cymodocea nodosa*	Macroalgae *Caulerpa prolifera*	Statistics
Dry bulk density (g cm^{-3})	0.9 ± 0.1 ^{a}	0.8 ± 0.1 ^{ab}	0.7 ± 0.1 ^{b}	0.3 ± 0.0 ^{c}	(K) $p < 0.001$
OM content (% dw)	3.78 ± 0.66 ^{a}	2.66 ± 0.33 ^{a}	6.06 ± 0.55 ^{b}	6.64 ± 0.29 ^{b}	(K) $p < 0.001$
TC content (% dw)	2.40 ± 0.31 ^{a}	2.65 ± 0.22 ^{a}	5.09 ± 0.11 ^{b}	4.80 ± 0.22 ^{b}	(A) $p < 0.001$
OC content (% dw)	1.48 ± 0.31 ^{a}	0.91 ± 0.13 ^{a}	1.45 ± 0.19 ^{ab}	2.01 ± 0.13 ^{b}	(K) $p < 0.001$
TN content (% dw)	0.121 ± 0.022 ^{a}	0.093 ± 0.015 ^{a}	0.168 ± 0.022 ^{ab}	0.233 ± 0.015 ^{b}	(K) $p < 0.001$
$CaCO_3$ content (% dw)	10.7 ± 1.0 ^{a}	11.4 ± 0.9 ^{a}	21.4 ± 0.3 ^{b}	21.4 ± 0.5 ^{b}	(K) $p < 0.001$
$\delta^{13}C$ (‰ vs. VPDB)	− 19.1 ± 0.6 ^{a}	− 16.7 ± 0.4 ^{a}	− 15.7 ± 0.5 ^{b}	− 17.0 ± 0.3 ^{a}	(K) $p < 0.001$
$\delta^{15}N$ (‰ vs. air)	4.45 ± 0.25	4.08 ± 0.22	3.78 ± 0.22	4.04 ± 0.17	(A) $p = 0.238$

The p-values of the one-way ANOVA (A) or Kruskal–Wallis (K) tests are shown. The alphabetic code indicates significant differences among habitats. OM: organic matter, TC: total carbon, OC: organic carbon, TN: total nitrogen

most superficial layer (16 cm) of the *Zostera noltei* core, suggesting intense mixing, yet it decreased with depth thereafter to constant values below 25 cm (Figure 3). In the *Cymodocea nodosa* core, excess ^{210}Pb decreased with depth down to 14 cm (Figure 3). The CF:CS model was applied to the upper 14 cm of the *C. nodosa* core and below the mixing layer (from 16 to 27 cm) of for the *Z. noltei* core, obtaining an MAS of 0.16 ± 0.03 g cm^{-2} y^{-1} for *C. nodosa* (SAR = 4.0 ± 0.9 mm y^{-1}) and 0.10 ± 0.01 g cm^{-2} yr^{-1} for *Z. noltei* (SAR = 2.4 ± 0.3 mm y^{-1}). For the *C. prolifera* and *S. maritimus* sites, the results of the ^{210}Pb analyses suggested intense mixing of the sediment (Figure 3), precluding the determination of the sedimentation rates for the last decades.

The two dating methods, ^{210}Pb and historical reconstruction, provided similar MAR and SAR for the cores in the *Zostera noltei* and *Cymodocea nodosa* habitats (Table 4). The MAR decreased twofold across the seascape decreasing with the elevation, from 0.24 g dw cm^{-2} y^{-1} in *S. maritimus* to 0.12 g dw cm^{-2} y^{-1} in the *Caulerpa prolifera* habitat, while the SAR showed the opposite pattern, ranging from 1.8 mm y^{-1} in the *Sporobolus maritimus* habitat to 3.5 mm y^{-1} in the *C. prolifera* one (Table 4). Mean OC and TN burial rates over the last century were related to elevation too. They showed a decreasing trend (15fold for OC and twofold for TN) with decreasing bed elevation (Table 4). The allochthonous source contribution to the sedimentary OM pool increased with the decreasing elevation, with mean contributions of 33% in *S. maritimus*, 38% *Z. noltei*, 53% *C. nodosa*, and 73% in *C. prolifera* (Table 4, Figure 5).

Discussion

This work presents the role of vegetated coastal habitats in the burial and storage of C and N along an elevation gradient seascape. The observed significant difference among habitats highlights the need for habitat-specific characterization to improve our prediction capacity of C and N stocks and sequestration rates in coastal systems. The results also suggest that the habitat position along the

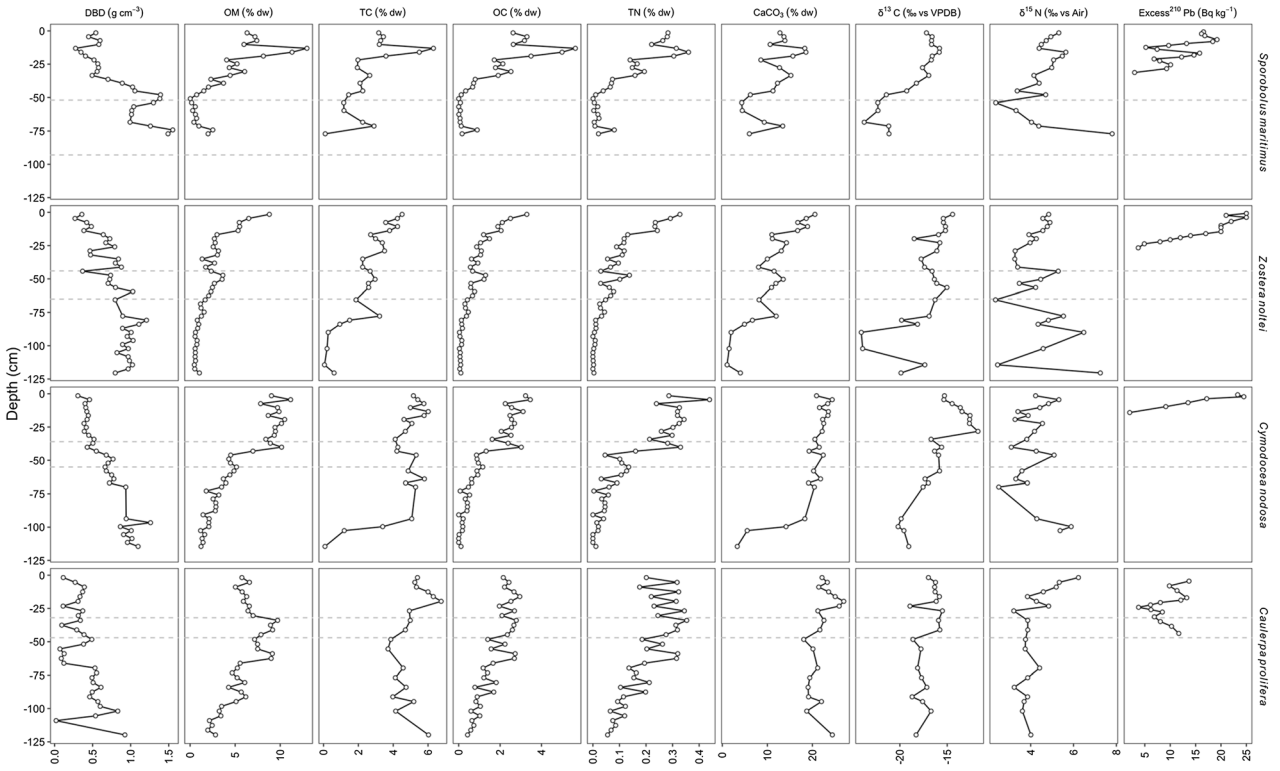

Figure 3. Sediment profiles for dry bulk density (DBD), organic matter (OM), total carbon (TC), organic carbon (OC), total nitrogen (TN), calcium carbonate ($CaCO_3$), ^{13}C signature ($\delta^{13}C$), ^{15}N signature ($\delta^{15}N$), and Excess ^{210}Pb, for the four vegetated habitats along the seascape: intertidal saltmarsh *Sporobolus maritimus*, intertidal seagrass *Zostera noltei*, subtidal seagrass *Cymodocea nodosa*, and subtidal macroalgae *Caulerpa prolifera*. The dashed lines delimit the depth at which a distinct layer (coarse grains, pebbles, and bioclasts) was observed in each habitat.

elevation gradient plausibly explains the observed spatial patterns. For the first time, the role of the rhizophytic macroalgae *Caulerpa prolifera* in sequestering carbon and nitrogen in the seabed sediments was evaluated, revealing that rhizophytic algae may contribute significantly to the C and N sequestration and storage in coastal systems.

The OC and TN burial rates for the last 100 y observed in *Z. noltei* and *S. maritimus* (Table 5) were in the same range than those reported for Cádiz Bay habitats by Jiménez-Arias and others (2020) and those reported in the neighbouring Ria Formosa lagoon (south Portugal) (Martins and others 2021). Sediment OC and TN stocks and burial rates, SAR, MAR, and allochthonous source contributions to sedimentary OM generally showed clear differences among vegetation habitats along the seascape. SAR varied along the elevation gradient with values decreasing with increasing elevation, whereas MAR showed the opposite pattern (Table 4). Sediment carbon stocks exhibited higher values in the subtidal seagrass and intertidal saltmarsh habitats and total nitrogen stocks were higher in subtidal than in intertidal habitats. OC and TN burial rates increased from the intertidal to the subtidal habitats (Table 4). The allochthonous source contribution to the sedimentary OM also showed a clear pattern with elevation, decreasing from the subtidal *C. prolifera* to the upper intertidal *S. maritimus*. Our initial hypothesis is only partially accepted as we expected the observed pattern in the allochthonous contribution, but it did not imply necessarily higher stocks and burial rates in the subtidal habitats. The type of sediment (denser) in the upper habitats may explain this unexpected pattern, since DBD is an important variable in the calculations of both stocks and burial rates. Taken together, our results demonstrate the need to use habitat-specific organic carbon and nitrogen stocks and burial rates if the OC and TN sink capacity of vegetated coastal habitats at the seascape level is to be more realistically estimated. They also suggest that elevation gradient and vegetation type may explain spatial patterns at the seascape level, as found in previous studies (for example, Kelleway and others 2017; Zhang and others 2017; Santos and others 2019; Jiménez-Arias and others 2020; de los Santos and others 2022).

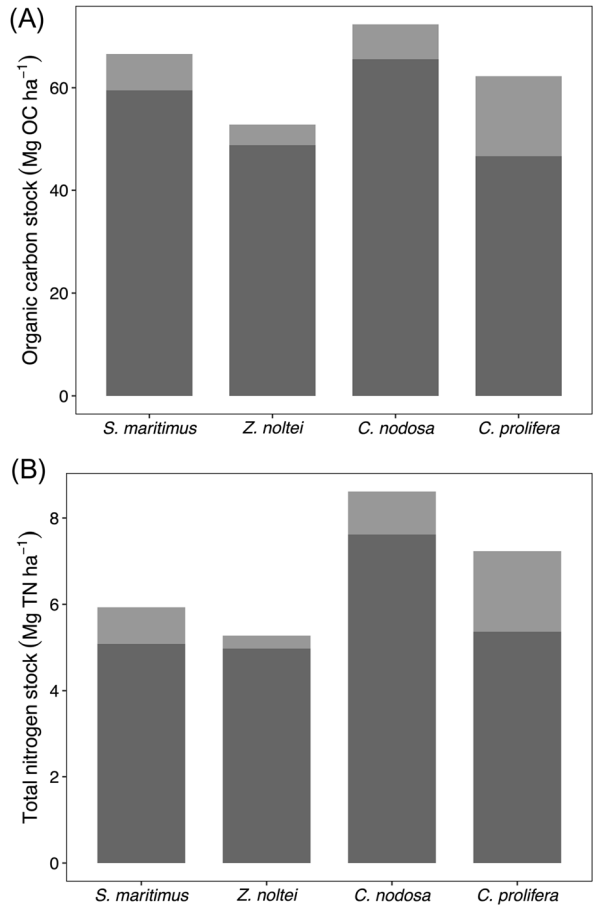

Figure 4. Stocks of organic carbon **A** and total nitrogen **B** in the upper 0.75 m (dark bar) and 1 m (dark + light bars) of sediment at the four vegetated habitats along the seascape: intertidal saltmarsh *Sporobolus maritimus*, intertidal seagrass *Zostera noltei*, subtidal seagrass *Cymodocea nodosa*, and subtidal macroalgae *Caulerpa prolifera*.

The spatial trend found on allochthonous OM contribution should be taken with caution, since it was estimated with stable isotope models that have clear limitations with the overlapping of macrophytes isotopic signatures and with changes in signature due to degradation processes (Geraldi and others 2019). In our case, the stable isotope models were reduced to one tracer due to the overlapping of δ^{15}N macrophyte signatures, limiting the number of sources included in the model for each habitat to two sources. Despite these limitations, the pattern observed agrees with our expectation of a higher contribution of the allochthonous OM in the subtidal than in the intertidal habitats. In any case, alternative methods to estimate the source of allochthonous contributions to the OC and TN stocks in the study area should be used in the future, such as metabarcoding of sedimentary DNA, which proved to be valid for identifying accurately macrophyte sources in the sediment (Reef and others 2017; Ortega and others 2020). SAR estimations were also subjected to an unknown level of uncertainty as sediment mixing was intense in the upper part of the cores collected from two of the sites and the reconstruction method assumes constant deposition since the tsunami event.

Overall, the vertical gradient along the seascape (that is, tidal position) seemed to have a great effect on sediment properties of vegetated coastal sediments. Subtidal habitats presented $CaCO_2$ contents two-fold higher ($\sim$ 20% dw) than intertidal ones. In the case of seagrasses, this might be influenced by the development of carbonate sediment facies as they host calcareous organisms, which became part of the substrate after death (Walker and Woelkerling 1988; Perry and Beavington-Penney 2005). In the study area, calcareous epiphytes such as encrusting coralline red algae, bryozoans, and foraminifera are normally found on the leaves of subtidal *C. nodosa*, but they are not so frequent on those of *Z. noltei* or *S. maritimus* (personal observation). Epiphytes are also unusual on *C. prolifera* fronds (Vergara and others 2012), therefore, the high $CaCO_3$ content observed in the sediment of this habitat must originate from adjacent *C. nodosa* meadows. Subtidal habitats also have more OM-rich sediments than intertidal ones, in part probably because of the deprivation of atmospheric air exchange in subtidal condition vs the enhanced low-tide OM decomposition in air-exposed sediments (Alongi and others 2001; Sasaki and others 2009). Higher allochthonous contribution in subtidal than intertidal habitats, due to higher hydroperiod, also contributes to the OM enrichment of sediments. Dry bulk density increases landward with elevation, which in combination with the OC and TN content patterns, explains the spatial patterns observed in the stocks, generally higher for *C. nodosa* and *S. maritimus* habitats, and burial rates, higher at *S. maritimus*.

Despite other macroalgae systems have been recommended to be included in the list of coastal ecosystems that act as marine carbon sinks, such as kelp forests (Hill and others 2015; Krause-Jensen and others 2016, 2018), rhizophytic macroalgae beds are overlooked in the literature. Unlike macroalgae growing on hard substrates, species of the genus *Caulerpa* have the ability to store carbon not only in their biomass but also in the soft substrate on which they commonly grow. In fact, our study demonstrates that the OC burial rates in *C. prolifera* habitats of Cádiz Bay (28 ± 6 g m^{-2} y^{-1}) were within the range reported for blue carbon

Table 4. Sedimentary Organic Carbon and Total Nitrogen Stocks (Top 1-m and Top 0.75-m), Sediment Accumulation Rates (SAR) Estimated Based on ^{210}Pb and Reconstruction Analysis, Depths at which Sediment is Aged 100 and 50 y, Burial Rates of Organic Carbon (OC) and Total Nitrogen (TN) (Over the Past 100 and 50 y), and Estimated Contributions of Allochthonous Organic Matter (Particulate Organic Matter) at the Vegetated Habitats Along the Seascape

Variable	Salt marsh *Sporobolus maritimus*	Seagrass *Zostera noltei*	Seagrass *Cymodocea nodosa*	Macroalgae *Caulerpa prolifera*
1-m organic carbon stock (Mg OC ha^{-1})	66.5	52.8	72.3	62.2
1-m total nitrogen stock (Mg TN ha^{-1})	5.9	5.3	8.6	7.2
0.75-m organic carbon stock (Mg OC ha^{-1})	59.5	48.8	65.5	46.6
0.75-m total nitrogen stock (Mg TN ha^{-1})	5.1	4.9	7.6	5.4
MAR (g dw cm^{-2} y^{-1})—^{210}Pb	n.a	0.103 ± 0.013	0.16 ± 0.03	n.a
MAR (g dw cm^{-2} y^{1})—reconstruction	0.244	0.323	0.130	0.117
Average MAR (g dw cm^{-2} y^{-1})	0.244	0.213 ± 0.156	0.145 ± 0.021	0.117
SAR (mm y^{-1})—^{210}Pb	n.a	2.4 ± 0.3	4.0 ± 0.9	n.a
SAR (mm y^{-1})—reconstruction	1.8	2.1	2.5	3.5
Average SAR (mm y^{-1})	1.8	2.2 ± 0.2	3.2 ± 1.1	3.5
Depth of 100 years (cm)	18	22	32	35
Depth of 50 years (cm)	9	11	16	18
OC burial (g OC m^{-2} y^{-1})—100 y	91 ± 31	44 ± 15	39 ± 6	28 ± 4
TN burial (g TN m^{-2} y^{-1})—100 y	7 ± 1	5 ± 2	5 ± 1	3 ± 1
OC burial (g OC m^{-2} y^{-1})—50 y	74 ± 9	56 ± 13	42 ± 7	29 ± 4
TN burial (g TN m^{-2} y^{-1})—50 y	7 ± 0	6 ± 1	5 ± 1	3 ± 1
Contribution allochthonous (%)	33	38	53	73

n.a. not available due to processes of sediment mixing.

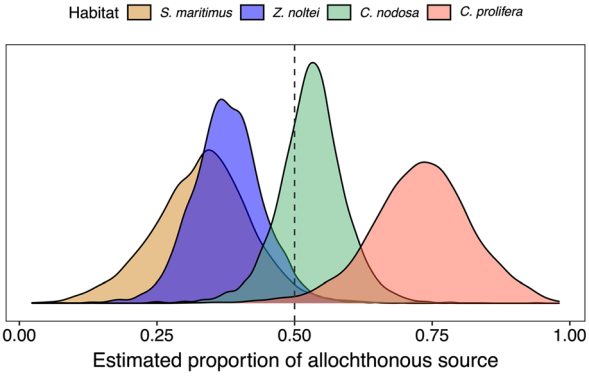

Figure 5. Estimated proportion of allochthonous (particulate organic matter) contribution to the sedimentary organic matter pool at the four vegetated habitats along the seascape: intertidal saltmarsh *Sporobolus maritimus*, intertidal seagrass *Zostera noltei*, subtidal seagrass *Cymodocea nodosa*, and subtidal macroalgae *Caulerpa prolifera*.

ecosystems (20–30 g m^{-2} y^{-1} for seagrasses, Arias-Ortiz 2019; and 18–1713 g m^{-2} y^{-1} for salt marshes, Mcleod and others 2011). *Caulerpa* beds in Cádiz Bay persist over the year with a seasonal pattern in their above- and below-ground biomass (Vergara and others 2012). This perennial nature means that they accumulate carbon in their sediments throughout the year. The high capacity of *C. prolifera* beds to sequester and store OC and TN relies in its high efficiency in trapping suspended particles, very similar to the capacity described for *C. nodosa* or even to one of the largest seagrass species such as *P. oceanica* (Hendriks and others 2011). Indeed, in Cádiz Bay, *C. prolifera* was the habitat with the highest sediment accumulation rate (3.5 mm y^{-1}, Table 4). This high capacity to trap and retain sediments is attributed to the very dense canopies that form this species and to its ability to root, which translates into a very complex frond structure and subterranean network of stolons and rhizoids (Vergara and others 2012). Sediments of *C. prolifera* presented high OM content (6.64% dw), similar to that of *C. nodosa* (6.06% dw), and comparable to values in this area reported by Vergara and others 2012 (10.5 ± 0.9% dw in *C. prolifera* sediment and 8.2 ± 0.9% dw in adjacent meadows of *C. nodosa*). The high OM content can be explained by the highly anoxic conditions typi-

Table 5. Compilation of Organic Carbon (OC) Stocks and Burial Rates for the Two Intertidal Vegetated Coastal Habitats From Cádiz Bay

Habitat	OC stock (Mg ha^{-1})	OC burial rate (g OC m^{-2} y^{-1})	TN stock (Mg ha^{-1})	TN burial rate (g TN m^{-2} y^{-1})	Source
Sporobolus maritimus	66.5	90.8 ± 31.1	5.9	7.0 ± 1.1	This study
	–	47.6 ± 7.4[1]	–	3.7 ± 0.8[1,2]	Jiménez-Arias and others (2020)
Zostera noltei	52.8	44.3 ± 14.6	5.3	4.8 ± 1.6	This study
	–	79.9 ± 27.2[1]	–	3.0 ± 0.8[1,2]	Jiménez-Arias and others (2020)

[1]*Rate obtained using a constant sediment accumulation rate of 3.6 mm* y^{-1} *for both Z. noltei and S. maritimus. Time frame for the calculations not given in the source.*
[2]*Value reported for organic nitrogen.*
Stocks and burial rates given for the top 1-m sediment and last 100 y, respectively, if not otherwise stated.

cal of these beds (Belando and others 2021), decreasing the efficiency of OM remineralization. On the other hand, the storage time for OC and TN may also be shorter in *Caulerpa* beds than in other vegetated habitats in the area mainly due to a lower protection capacity of their canopies. Firstly, the canopy structure of *Caulerpa* is much looser than those of seagrasses or saltmarsh species, likely not providing sufficient stability during high energy events, and eventually, leading to erosion and remineralization of the OC and TN stored in their sediments. Secondly, unlike other macroalgae, the order of Caulerpales does not contain cellulose (Kloareg and Quatrano 1988), which makes them labile matter with low C:N ratios. Consequently, the combination of anoxic conditions, poor protection by the canopies, and the labile nature of *Caulerpa* biomass likely explains the lower contribution of autochthonous OM to the sediment OM pool of this habitat.

The presence of pebbles and bioclasts points to a high-energy event to explain the presence of a distinctive layer observed in the cores of the four habitats. The 1755 Lisbon earthquake (Richter magnitude of 8.5—9) triggered an extremely large tsunami that hit the western and southern shores of the Iberian Peninsula. Exceptional events, like tsunamis, leave recognizable signals in sedimentary deposits. In Cádiz Bay, the propagation of the tsunamigenic wave, and the consequent flooding, came from the NW, entering the lagoon through the sand bar that separates the open sea from the inner bay (where the study area is located, Dabrio and others 1998). The effects of tsunamis on the depositional regime of the Cádiz Bay littoral include the erosion of pre-existing deposits and subsequent transport and re-sedimentation (Gutiérrez-Más and others 2009). The fossils found in our cores are from a scleractinian coral species (*C. caespitosa*) that creates large true reefs in present-day Mediterranean Sea and had generated large fossil banks in the Atlantic (for example, Zibrowius 1983). Thus, its presence in the inner bay could be due to the re-sedimentation of the material transported by the tsunamigenic wave. A dead bank of this coral species was also recently found embedded in a matte of *Posidonia oceanica* (Monnier and others 2021).

The OC and TN stocks and burial rates here presented allow us to obtain the first rough estimated accounts of sedimentary organic carbon and nitrogen burial and storage capacity in the vegetated coastal habitats of inner Cádiz Bay, yet these estimates should be considered with caution given they are based on data from 1 core per habitat. In addition, we are not fully certain that the full retrieved sediment core at each sampling point represents the present habitat in the deeper layers. Despite this limitation, we believe it is still meaningful to associate the carbon and nitrogen stocks with the current habitats because the sediment layer that contributes most to the estimated stocks is the surface layer, where most of the organic matter accumulates and which is also the most recent layer. If the habitat distribution many years ago was different from today, the organic matter deposited and buried at that time might not have a significant contribution to the total measured stocks.

Considering the most updated areas covered by the four habitats, we estimate an organic carbon and total nitrogen stocks in the upper 1-m sediment layer of 303,000 Mg OC and 32,100 Mg TN for the whole inner bay, with the largest contribution by salt marsh (36%) and *Caulerpa prolifera* (30%) habitats (Table 6). The total estimated OC

Table 6. Estimation of the Organic Carbon (OC) and Total Nitrogen (TN) Stocks (Upper 1-m Sediment Layer) and Burial Rates (100 y) by the Coastal Vegetated Habitats in the Inner Cádiz Bay

Habitat	Area (ha)	OC stock (Mg OC)	TN stock (Mg TN)	OC burial rate (Mg OC y^{-1})	TN burial rate (Mg TN y^{-1})
Sporobolus maritimus	1,659	110,000 (36%)	9,800 (31%)	1,500	120
Zostera noltei	858	45,000 (15%)	4,500 (14%)	380	41
Cymodocea nodosa	790	57,000 (19%)	6,800 (21%)	310	36
Caulerpa prolifera	1,466	91,000 (30%)	11,000 (33%)	410	45
All habitats	4,772	303,000	32,100	2600	242

The contribution of each habitat to the total OC or TN stock is giving as percentage. The area for each habitat was retrieved from Muñoz-Pérez and Sánchez de LaMadrid (1994) and d'El Rei (2009).

and TN burial capacity is of 2600 Mg OC $y^{-1}$and 240 Mg TN y^{-1}, respectively (Table 6). These estimations do not consider spatial variability in stocks and burial rates within the system, which has been observed in many other wetlands (for example, Ricart and others 2020; Martins and others 2021). In Cádiz Bay, the existing variability in hydrodynamics within the inner bay (del Río and others 2012; Zarzuelo and others 2017) is expected to affect the OC and TN storage and sequestration capacity by the vegetated coastal habitats, so it requires further investigation to obtain precise estimations. Additionally, clam harvesting, which is widespread in the intertidal areas of Cádiz Bay, as well as other physical impacts (for example, boating and anchoring or coastal constructions), could have an impact on the present carbon and nitrogen stocks as described in other similar systems (for example, Román and others 2022). Future investigations should focus on spatial variability of organic carbon and total nitrogen stocks within the inner Cádiz Bay to obtain more precise estimates. Despite *C. nodosa* and *Z. noltei* meadows in Andalusia have been considered to have ''an almost negligible contribution to the Andalusian blue carbon'' (Mateo and others 2018), we consider that our estimation of more than 100 Gg OC stored in the seagrass habitats of Cádiz Bay, with an annual burial rate of 690 Mg OC y^{-1} (equivalent to 2,500 Mg of CO_2 sequestered per year) is significant at the regional level and contributes to the mitigation of climate change. Seagrass ecosystems provide many other ecosystem services such as water purification, biodiversity support, coastal protection, and cultural values (Barbier and others 2011), so their valuation should consider not only the blue carbon storage capacity, but all the ecosystem services they provide.

ACKNOWLEDGEMENTS

This study was funded by International Campus of Excellence of the Sea (CEIMAR) though the program Young Researcher CEIMAR Research Projects Call 2018 (project CADYCCO), and additional funding from the Portuguese FCT—Foundation for Science and Technology (grant and contract numbers: UIDP/04326/2020, LA/P/0101/2020, 2020.03825.CEECIND, and 2020.06996.BD). Authors are thankful to Pedro Costa (University of Lisbon) and Juan Ignacio Santisteban (Complutense University of Madrid) for the help with the identification of the corals. Funding was provided to P.M. through an Australian Research Council LIEF Project (LE170100219). The International Atomic Energy Agency is grateful for the support provided to its Marine Environment Laboratories by the Government of the Principality of Monaco.

Declarations

Conflict of interest The authors declare that they have no conflict of interest.

REFERENCES

Alongi DM, Wattayakorn G, Pfitzner J, Tirendi F, Zagorskis I, Brunskill GJ, Davidson A, Clough BF. 2001. Organic carbon accumulation and metabolic pathways in sediments of mangrove forests in southern Thailand. Marine Geol 179(1–2):85–103. https://doi.org/10.1016/S0025-3227(01)00195-5.

Alvarez O, Izquierdo A, Tejedor B, Mañanes R, Tejedor L, Kagan BA. 1999. The influence of sediment load on tidal dynamics, a case study: Cádiz Bay. Estuar Coast Shelf Sci 48(4):439–450. https://doi.org/10.1006/ecss.1998.0432.

Appleby PG, Oldfield F. 1978. The calculation of lead-210 dates assuming a constant rate of supply of unsupported ^{210}Pb to the sediment. Catena 5(1):1–8. https://doi.org/10.1016/S0341-8162(78)80002-2.

Arias-Ortiz A. 2019. Carbon sequestration rates in coastal Blue Carbon ecosystems: A perspective on climate change mitigation. Universitat Autònoma de Barcelona.

Arias-Ortiz A, Masqué P, Garcia-Orellana J, Serrano O, Mazarrasa I, Marbà N, Lovelock CE, Lavery PS, Duarte CM. 2018. Reviews and syntheses: 210Pb-derived sediment and carbon accumulation rates in vegetated coastal ecosystems – setting the record straight. Biogeosciences 15(22):6791–6818. https://doi.org/10.5194/bg-15-6791-2018.

Barbier EB, Hacker SD, Kennedy C, Koch EW, Stier AC, Silliman BR. 2011. The value of estuarine and coastal ecosystem services. Ecol Monogr 81(2):169–193. https://doi.org/10.1890/10-1510.1.

Belando MD, Bernardeau-Esteller J, Paradinas I, Ramos-Segura A, García-Muñoz R, García-Moreno P, Marín-Guirao L, Ruiz JM. 2021. Long-term coexistence between the macroalga *Caulerpa prolifera* and the seagrass *Cymodocea nodosa* in a Mediterranean lagoon. Aquat Bot 173:103415. https://doi.org/10.1016/j.aquabot.2021.103415.

Bridgham SD, Megonigal JP, Keller JK, Bliss NB, Trettin C. 2006. The carbon balance of North American wetlands. Wetlands 26:889–916. https://doi.org/10.1672/0277-5212(2006)26[889:TCBONA]2.0.CO;2.

Brun FG, Vergara JJ, Pérez-Lloréns JL, Ramírez C, Morris P. 2015. Diversidad de angiospermas marinas en la bahía de Cádiz: Redescubriendo a *Zostera marina*. Chron Nat 5:45–56.

Bulmer RH, Stephenson F, Jones HFE, Townsend M, Hillman JR, Schwendenmann L, Lundquist CJ. 2020. Blue carbon stocks and cross-habitat subsidies. Front Marine Sci 7:380. https://doi.org/10.3389/fmars.2020.00380.

Carrasco M, López-Ramirez JA, Benavente J, López-Aguayo F, Sales D. 2003. Assessment of urban and industrial contamination levels in the bay of Cádiz SW Spain. Marine Pollut Bull 46(3):335–345. https://doi.org/10.1016/S0025-326X(02)00420-4.

Cole SG, Moksnes P-O. 2016. Valuing multiple eelgrass ecosystem services in Sweden: fish production and uptake of carbon and nitrogen. Front Marine Sci 2:121. https://doi.org/10.3389/fmars.2015.00121.

d'El Rei D. 2009. Teledetección de hábitats bentónicos en la Bahía de Cádiz, España. MSc Thesis, University of Cádiz. http://hdl.handle.net/10498/14120.

Dabrio CJ, Goy JL, Zazo C. 1998. The record of the tsunami produced by the 1755 Lisbon earthquake in Valdelagrana spit (Gulf of Cádiz, southern Spain). Geogaceta 23:31–34.

de Andrés M, Barragán JM, García Sanabria J. 2018. Ecosystem services and urban development in coastal social-ecological systems: the bay of Cádiz case study. Ocean Coast Manage 154:155–167. https://doi.org/10.1016/j.ocecoaman.2018.01.011.

de los Santos CB, Lahuna F, Silva A, Freitas C, Martins M, Carrasco AR, Santos R. 2022. Vertical intertidal variation of organic matter stocks and patterns of sediment deposition in a mesotidal coastal wetland. Estuar Coast Shelf Sci 272:107896. https://doi.org/10.1016/j.ecss.2022.107896.

Del Río L, Plomaritis TA, Benavente J, Valladares M, Ribera P. 2012. Establishing storm thresholds for the Spanish Gulf of Cádiz coast. Geomorphology 143–144:13–23. https://doi.org/10.1016/j.geomorph.2011.04.048.

Duarte CM, Marbà N, Gacia E, Fourqurean JW, Beggins J, Barrón C, Apostolaki ET. 2010. Seagrass community metabolism: Assessing the carbon sink capacity of seagrass meadows. Glob Biogeochem Cycl 24:GB4032. https://doi.org/10.1029/2010GB003793.

Duarte CM, Middelburg JJ, Caraco N. 2005. Major role of marine vegetation on the oceanic carbon cycle. Biogeosciences 2:1–8. https://doi.org/10.5194/bg-2-1-2005.

Geraldi NR, Ortega A, Serrano O, Macreadie PI, Lovelock CE, Krause-Jensen D, Kennedy H, Lavery PS, Pace ML, Kaal J, Duarte CM. 2019. Fingerprinting blue carbon: rationale and tools to determine the source of organic carbon in marine depositional environments. Front Marine Sci 6:263. https://doi.org/10.3389/fmars.2019.00263.

Gutiérrez-Mas JM, López-Arroyo J, Morales JA. 2009. Recent marine lithofacies in Cádiz Bay (SW Spain). Sediment Geol 218(1–4):31–47. https://doi.org/10.1016/j.sedgeo.2009.04.002.

Hendriks IE, Bouma TJ, Morris EP, Duarte CM. 2010. Effects of seagrasses and algae of the *Caulerpa* family on hydrodynamics and particle-trapping rates. Marine Biol 157(3):473–481. https://doi.org/10.1007/s00227-009-1333-8.

Hill R, Bellgrove A, Macreadie PI, Petrou K, Beardall J, Steven A, Ralph PJ. 2015. Can macroalgae contribute to blue carbon? An Australian perspective. Limnol Oceanogr 60(5):1689–1706. https://doi.org/10.1002/lno.10128.

Howard J, Hoyt S, Isensee K, Pidgeon E, Telszewski M. 2014. Coastal blue carbon: Methods for assessing carbon stocks and emissions factors in mangroves, tidal salt marshes, and seagrass meadows (p. 186) [Manual]. Conservation International, Intergovernmental Oceanographic Commission of UNESCO, International Union for Conservation of Nature.

Huxham M, Whitlock D, Githaiga M, Dencer-Brown A. 2018. Carbon in the coastal seascape: how interactions between mangrove forests, seagrass meadows and tidal marshes influence carbon storage. Curr for Rep 4:101–110. https://doi.org/10.1007/s40725-018-0077-4.

Jiménez-Arias JL, Morris E, Rubio-de-Inglés MJ, Peralta G, García-Robledo E, Corzo A, Papaspyrou S. 2020. Tidal elevation is the key factor modulating burial rates and composition of organic matter in a coastal wetland with multiple habitats. Sci Total Environ 724:138205. https://doi.org/10.1016/j.scitotenv.2020.138205.

Kelleway JJ, Saintilan N, Macreadie PI, Baldock JA, Ralph PJ. 2017. Sediment and carbon deposition vary among vegetation assemblages in a coastal salt marsh. Biogeosciences 4(16):3763–3779. https://doi.org/10.5194/bg-14-3763-2017.

Kennedy H, Beggins J, Duarte CM, Fourqurean JW, Holmer M, Marbà N, Middelburg JJ. 2010. Seagrass sediments as a global carbon sink: Isotopic constraints. Glob Biogeochem Cycl 24:GB4026. https://doi.org/10.1029/2010GB003848.

Kennedy P, Kennedy H, Papadimitriou S. 2005. The effect of acidification on the determination of organic carbon, total nitrogen and their stable isotopic composition in algae and marine sediment. Rapid Commun Mass Spectrom 19(8):1063–1068. https://doi.org/10.1002/rcm.1889.

Kloareg B, Quatrano RS. 1988. Structure of the cell walls of marine algae and ecophysiological functions of the matrix polysaccharides. Oceanogr Marine Biol Annu Rev 26:259–315.

Krause-Jensen D, Duarte CM. 2016. Substantial role of macroalgae in marine carbon sequestration. Nat Geosci 9(10):737–742. https://doi.org/10.1038/ngeo2790.

Krause-Jensen D, Lavery P, Serrano O, Marbà N, Masque P, Duarte CM. 2018. Sequestration of macroalgal carbon: The

elephant in the blue carbon room. Biol Lett 14(6):20180236. https://doi.org/10.1098/rsbl.2018.0236.

Krishnaswami S, Lal D, Martin JM, Meybeck M. 1971. Geochronology of lake sediments. Earth Planet Sci Lett 11:407–414.

Macreadie PI, Anton A, Raven JA, Beaumont N, Connolly RM, and others 2019. The future of blue carbon science. Nat Commun 10(1):3998. https://doi.org/10.1038/s41467-019-11693-w.

Martins M, de los Santos CB, Masqué P, Carrasco AR, Veiga-Pires C, Santos R. 2022. Carbon and nitrogen stocks and burial rates in intertidal vegetated habitats of a mesotidal coastal lagoon. Ecosystems 25:372–386. https://doi.org/10.1007/s10021-021-00660-6.

Mateo MÁ, Díaz-Almela E, Piñeiro-Juncal N, Leiva-Dueñas C, Giralt-Romeu S, Marco-Méndez C. 2018. Carbon stocks and fluxes associated to Andalusian seagrass meadows. Deliverable c1: results report. (p. 95). CEAB-CSIC.

Mateo MÁ, Romero J, Pérez M, Littler MM, Littler DS. 1997. Dynamics of millenary organic deposits resulting from the growth of the Mediterranean seagrass *Posidonia oceanica*. Estuar Coast Shelf Sci 44:103–110. https://doi.org/10.1006/ecss.1996.0116.

Mcleod E, Chmura GL, Bouillon S, Salm R, Björk M, Duarte CM, Lovelock CE, Schlesinger WH, Silliman BR. 2011. A blueprint for blue carbon: toward an improved understanding of the role of vegetated coastal habitats in sequestering CO_2. Front Ecol Environ 9:552–560. https://doi.org/10.1890/110004.

Monnier B, Lehmann L, Sartoretto S, Pergent-Martini C, Mateo MÁ, Pergent G. 2021. Long-term dynamics of a *Cladocora caespitosa* bank as recorded by a *Posidonia oceanica* millenary archive. Estuar Coast Shelf Sci 256:107378. https://doi.org/10.1016/j.ecss.2021.107378.

Morris EP, Peralta G, Benavente J, Freitas R, Rodrigues A, Quintino V, Alvarez O, Valcárcel-Pérez N, Vergara J, Hernández I, Pérez-Lloréns J. 2009. *Caulerpa prolifera* stable isotope ratios reveal anthropogenic nutrients within a tidal lagoon. Marine Ecol Prog Ser 390:117–128. https://doi.org/10.3354/meps08184.

Mueller P, Ladiges N, Jack A, Schmiedl G, Kutzbach L, Jensen K, Nolte S. 2019. Assessing the long-term carbon-sequestration potential of the semi-natural salt marshes in the European Wadden Sea. Ecosphere 10(1):e02556. https://doi.org/10.1002/ecs2.2556.

Nellemann C, Corcoran E, Duarte CM, Valdés L, De Young C, Fonseca L, Grimsditch G. 2009. Blue carbon - the role of healthy oceans in binding carbon, United Nations Environment.

Ortega A, Geraldi NR, Duarte CM. 2020. Environmental DNA identifies marine macrophyte contributions to Blue Carbon sediments. Limnol Oceanogr 65(12):3139–3149. https://doi.org/10.1002/lno.11579.

Parnell AC, Phillips DL, Bearhop S, Semmens BX, Ward EJ, Moore JW, Jackson AL, Grey J, Kelly DJ, Inger R. 2013. Bayesian stable isotope mixing models. Environmetrics 24(6):387–399. https://doi.org/10.1002/env.2221.

Parnell AC. 2019. Package ''simmr'': a stable isotope mixing model. [R programming language].

Peng Y, Liu D, Wang Y, Richard P, Keesing JK. 2018. Analyzing biases of nitrogen contents and $\delta^{15}N$ values arising from acidified marine sediments with different $CaCO_3$ concentrations. Acta Oceanol Sin 37(8):1–5. https://doi.org/10.1007/s13131-018-1188-2.

Pennings SC, Callaway RM. 1992. Salt marsh plant zonation: the relative importance of competition and physical factors. Ecology 73(2):681–690. https://doi.org/10.2307/1940774.

Peralta G, Godoy O, Egea LG, de los Santos CB, Jiménez-Ramos R, Lara M, Brun FG, Hernández I, Olivé I, Vergara JJ, González-Ortiz V, Moreno-Marín F, Morris EP, Villazán B, Pérez-Lloréns JL. 2021. The morphometric acclimation to depth explains the long-term resilience of the seagrass *Cymodocea nodosa* in a shallow tidal lagoon. J Environ Manage 299:113452. https://doi.org/10.1016/j.jenvman.2021.113452.

Perry CT, Beavington-Penney SJ. 2005. Epiphytic calcium carbonate production and facies development within sub-tropical seagrass beds, Inhaca Island Mozambique. Sediment Geol 174(3–4):161–176. https://doi.org/10.1016/j.sedgeo.2004.12.003.

R Core Team. 2021. R: A language and environment for statistical computing. R Foundation for Statistical Computing, Vienna, Austria. https://www.R-project.org/.

Rabalais NN, Turner RE, Díaz RJ, Justić D. 2009. Global change and eutrophication of coastal waters. ICES J Marine Sci 66:1528–1537. https://doi.org/10.1093/icesjms/fsp047.

Reef R, Atwood TB, Samper-Villarreal J, Adame MF, Sampayo EM, Lovelock CE. 2017. Using eDNA to determine the source of organic carbon in seagrass meadows. Limnol Oceanogr 62(3):1254–1265. https://doi.org/10.1002/lno.10499.

Ricart AM, York PH, Bryant CV, Rasheed MA, Ierodiaconou D, Macreadie PI. 2020. High variability of blue carbon storage in seagrass meadows at the estuary scale. Sci Rep 10(1):5865. https://doi.org/10.1038/s41598-020-62639-y.

Román M, de los Santos CB, Román S, Santos R, Troncoso JS, Vázquez E, Olabarria C. 2022. Loss of surficial sedimentary carbon stocks in seagrass meadows subjected to intensive clam harvesting. Marine Environ Res 175:105570. https://doi.org/10.1016/j.marenvres.2022.105570.

Romero JA, Comín FA, García C. 1999. Restored wetlands as filters to remove nitrogen. Chemosphere 39:323–332. https://doi.org/10.1016/S0045-6535(99)00113-7.

Sánchez-Cabeza JA, Masqué P, Ani-Ragolta I. 1998. ^{210}Pb and ^{210}Po analysis in sediments and soils by microwave acid digestion. J Radioanal Nucl Chem 227:19–22.

Muñoz-Pérez JL, Sánchez de La Madrid Rey A. 1994. El medio físico y biológico en la Bahia de Cádiz: Saco interior. Centro de Investigación y Cultivo de Especies Marinas ''El Toruño''.

Santos R, Duque-Núñez N, de los Santos CB, Martins M, Carrasco AR, Veiga-Pires C. 2019. Superficial sedimentary stocks and sources of carbon and nitrogen in coastal vegetated assemblages along a flow gradient. Sci Rep 9(1):610. https://doi.org/10.1038/s41598-018-37031-6.

Sasaki A, Hagimori Y, Nakatsubo T, Hoshika A. 2009. Tidal effects on the organic carbon mineralization rate under aerobic conditions in sediments of an intertidal estuary. Ecol Res 24(4):723–729. https://doi.org/10.1007/s11284-008-0545-6.

Smale DA, Moore PJ, Queirós AM, Higgs ND, Burrows MT. 2018. Appreciating interconnectivity between habitats is key to blue carbon management. Front Ecol Environ 16:71–73. https://doi.org/10.1002/fee.1765.

Sousa AI, Santos DB, da Silva EF, Sousa LP, Cleary DFR, Soares AMVM, Lillebø AI. 2017. 'Blue Carbon' and nutrient stocks of salt marshes at a temperate coastal lagoon (Ria de Aveiro, Portugal). Sci Rep 7(1):41225. https://doi.org/10.1038/srep41225.

Sousa A, da Silva J, Azevedo A, Lillebo A. 2019. Blue carbon stock in *Zostera noltei* meadows at Ria de Aveiro coastal lagoon (Portugal) over a decade. Sci Rep 9:14387. https://doi.org/10.1038/s41598-019-50425-4.

Vergara JJ, García-Sánchez MP, Olivé I, García-Marín P, Brun FG, Pérez-Lloréns JL, Hernández I. 2012. Seasonal functioning and dynamics of *Caulerpa prolifera* meadows in shallow areas: An integrated approach in Cádiz Bay Natural Park. Estuar Coast Shelf Sci 112:255–264. https://doi.org/10.1016/j.ecss.2012.07.031.

Walker D, Woelkerling W. 1988. Quantitative study of sediment contribution by epiphytic coralline red algae in seagrass meadows in Shark Bay, Western Australia. Marine Ecol Prog Ser 43:71–77. https://doi.org/10.3354/meps043071.

Watanabe K, Yoshida G, Hori M, Umezawa Y, Moki H, Kuwae T. 2020. Macroalgal metabolism and lateral carbon flows can create significant carbon sinks. Biogeosciences 17:2425–2440. https://doi.org/10.5194/bg-17-2425-2020.

Zarzuelo C, López-Ruiz A, Díez-Minguito M, Ortega-Sánchez M. 2017. Tidal and subtidal hydrodynamics and energetics in a constricted estuary. Estuar Coast Shelf Sci 185:55–68. https://doi.org/10.1016/j.ecss.2016.11.020.

Zhang T, Chen H, Cao H, Ge Z, Zhang L. 2017. Combined influence of sedimentation and vegetation on the soil carbon stocks of a coastal wetland in the Changjiang estuary. Chin J Oceanol Limnol 35(4):833–843. https://doi.org/10.1007/s00343-017-6054-0.

Zibrowius H. 1983. Nouvelles données sur la distribution de quelques scléractiniaires ''méditerranéens'' à l'est et à l'ouest du détroit de Gibraltar. Rapports Et Procès-Verbaux Des Réunions De La Commission Internationale Pour L'exploration Scientifique De La Mer Méditerranée 28:307–309.

Zubia M, Draisma SGA, Morrissey KL, Varela-Álvarez E, De Clerck O. 2020. Concise review of the genus *Caulerpa* J.V. Lamouroux. J Appl Phycol 32(1):23–39. https://doi.org/10.1007/s10811-019-01868-9.

Springer Nature or its licensor (e.g. a society or other partner) holds exclusive rights to this article under a publishing agreement with the author(s) or other rightsholder(s); author self-archiving of the accepted manuscript version of this article is solely governed by the terms of such publishing agreement and applicable law.